# Beta Radiation Response of SIRAD® Colorimetric Dosimeter vs. Theoretical Calculation of Beta Dose in the 5 to 25 rad Range.

A Thesis submitted
to the Faculty of the Graduate School of Arts and Sciences of
Georgetown University
in partial fulfillment of the requirements for the
degree of
Master of Science in Health Physics

By

Sisay Abegaz

Washington, DC
December, 2011

## ABSTRACT

SIRAD® family of colorimetric dosimeters has been calibrated to read gamma ray doses in the 1 to 1,000 rad range. Their use has now been established and tested by the Department of Homeland Security (DHS) to meet the DHS specifications for emergency estimation of personal gamma dose. These dosimeters are being distributed in Japan in the hundreds of thousands to citizens, to alleviate concerns about receiving exposures dangerous to health from the emissions of the Fukushima reactors. They have been approved for distribution to responders and citizens in the United States, but so far have been received by only a limited proportion of the U.S. population.

The goal of this thesis project is to test the response of SIRAD dosimeters to beta radiation. In order to test the beta response of these colorimetric dosimeters, both the card-size RADTriage and the postage-stamp-size RADSticker dosimeters were exposed for a known number of days in close proximity to the beta radiation emitted from uranium-glazed plates. These plates emit mainly beta radiation, and only a very small amount of gamma or bremmstrahlung x-rays. The numbers of days of exposure for these dosimeters were selected to obtain darkness related to gamma exposures in at least the 5 to 25rad range.

The observed human eye readings were then compared to calculated beta ray doses by two methods: 1) calculations using the VARSKIN code and 2) a direct method of calculating the beta ray dose which triply integrates over beta spectra emitted from the uranium glazes. Although results are obtained with a limited number of dosimeters, they do indicate that more detailed experiments will show that the SIRAD families of dosimeters have an adequate response to beta radiation so that they may be used for determining both beta and gamma doses under emergency conditions.

**ACKNOWLEDGEMENTS**

I would like to thank Dr. Allen Brodsky of Georgetown University for his invaluable support in every part of this work and Mr. Ray Johnson of Dade Moeller Radiation Safety Academy for letting me used some of the uranium glazed saucer plates from his training material collection. I also thank Dr. Marko Moscovitch, and Dr. Gary Phillips of Georgetown University, Dr. Gordhan N Patel of JP Laboratories and Dr. Stephen A. McGuire for their support and inspiration during the development and completion of the thesis. I would like to extend my great appreciation to Oak ridge National Laboratory for granting me the permission to use the code VARSKIN-3.

I would also like to thank my wife and my daughter for their unwavering support during the whole period.

TABLE OF CONTENT

Abstract ……..…… *ii*

Acknowledgments ……..…… *iii*

Table of content…….……. *iv*

List of Tables ……..... *vi*

List of Figures ……..... *vi*

1. Introduction

1.1 Goal of the study…….….. 1
1.2 General Approach …… 2

2. Background

2.1 Importance of beta particle dosimetry in radiation protection …. 3

2.2 Methods of measuring beta radiation dose …… 5

2.3 Methods of calculating beta dose from geometric distributions

of beta emitters ……..……... 7

2.4 Colorimetric dosimeters ……. 10

2.5 Uranium glazed plates as sources of beta radiation …….……. 12

2.6 Unattenuated beta energy spectra of nuclides from uranium glaze…..…… 14

3. Methods Used In This Thesis

3.1 Dose measurements …….…….…… 14

3.2 Methods of calculating beta dose from uranium glazed plates ……. 16

3.3 Absorption measurements to characterize the emitted spectrum

from uranium glazed plates …….. 18

3.4 Statistical tests on the uniformity of uranium glaze……..…..…… 19

3.5 Interpretation of darkening of SIRAD dosimeters in terms absorbed dose …… 19

4. Results…….. 20

5. Discussion…….……. 21

6. Conclusions …….…….……. 23

Tables…….…….…….. 25

Figures……..…….…….…… 28

Exhibit A- Calculation of beta dose by direct integration of beta doses (for comparison to VARSKIN calculated results) by Professor Brodsky …….. 34

References Cited…… 36

## LIST OF TABLES

Table 1. Results of color change readings for RADSticker and RADTriage vs. calculated doses 25
Table 2. Data for testing uniformity of uranium glaze 26

Table 3. Absorption data on beta intensities by layers of paper, for both GM and NaI thin window detectors 27

Table 4. Statistical variance analysis of data values based on tables 1 and 2 above 27

Table 5. Beta spectrum data used in VARSKIN calculation. Data entered into VARSKIN code for calculations of dose 28

## LIST OF FIGURES

Figure 1. The two commercially available SIRAD dosimeters (RADSticker and RADTriage-FIT) 29

Figure 2. Photograph of the stamp-size RADSticker placed at the center of a uranium-glazed dish 29

Figure 3. Beta ray spectra of Protactinium-234 and Protactinium-234m 30

Figure 4. Partial decay chain of Uranium-238 30

Figure 5. Picture of NaI and Geiger counters placed over uranium glaze 31

Figure 6a. Beta absorption plot versus paper thickness, with GM placed over the thickness added to the plate. 31

Figure 6b. Beta absorption plot vs. paper thickness using thin NaI detector 32

Figure 7. Range in low Z materials vs. electron energies from reference. 32
Figure 8. Photograph of beta-exposed RADSticker and RADTriage 33

Figure 9a. Photographs of VARSKIN input screen 33

Figure 9b. Photograph of VARSKIN output screen 33

# 1. INTRODUCTION

## 1.1 Goal of the study

In this thesis, SIRAD® colorimetric dosimeters (the self-indicating radiation dosimeters developed by Dr. Gordhan Patel at JP Laboratories (Riel et al. 2006)) are tested for their use as beta radiation dosimeters using uranium-glazed plates as sources of beta radiation. These dosimeters have previously been tested and approved for emergency measurements of gamma radiation (Klemic et al. 2007).

Colorimetric dosimeters are chemical dosimeters with a visible color change (or darkening) associated with exposure to ionizing radiation. Historically, colorimetric dosimeters have been used for measuring higher dose values by the military and emergency responders. The SIRAD family of dosimeters uses diacetylene monomers that have been developed to change color as they increase in polymerization with increasing radiation exposure. They have evolved and their sensitivity has increased to include measuring doses in the range below the annual public and occupational limits established by regulatory bodies. However, it is important under emergency conditions that members of the public are not unduly frightened by measurements of the low acceptable doses and dose rates that are designed for peacetime conditions to limit lifetime exposures (Brodsky 2010).

SIRAD colorimetric dosimeters have recently gained popularity for their use as dosimeters of convenience for emergency responders and the general public. In the recent Japanese Fukushima Daiichi nuclear power plant incident, SIRAD dosimeters were chosen for use by different news reporter crews, the military and civilian emergency responders who travelled to Japan. They have also been made available in large quantities for purchase by members of the Japanese public.

## 1.2 **General Approach**

SIRAD dosimeters were placed on uranium glazed saucer plates and left for days to accumulate doses in the expected range of 5-25 rad. Color changes in the center strips of these dosimeters were interpreted as dose by matching the color changes to adjacent squares of varying darkness that were labeled to correspond to the respective received doses. Pictures of these dosimeters are included in the Figures of this document.

The count rate and beta ray dose at the surface of the plate were measured using a Geiger counter and a NaI scintillation detector. The values read by observing color changes (or darkness for color blind individuals) of the SIRAD dosimeters are compared with beta ray absorbed doses in the dosimeters (which would closely represent skin doses if the dosimeters were worn on the surfaces of skin). The beta doses read from the dosimeters were then compared against a dose obtained using two calculation methods. Both calculation methods used count rates in a defined open window area of a Geiger counter, which were also checked with a thin-window, 1-mm-thick, NaI detector. These count rates were used to determine the fluence rates of beta rays entering the centers of the exposed SIRAD dosimeters. These fluence rates were used to calculate the dose by: 1) using the VARSKIN-3 code (Durham et al. 1992; Sherbini et al. 2008); and 2) also using direct dose calculations obtained from triply integrating betas incident upon the centers of the dosimeters over elements of the glaze surface in circular coordinates, over the energy spectrum of the betas, and as weighted over the mass stopping powers as a function of energy. The direct dose calculations of 2) are necessarily presented separately in Exhibit A, which in MATHCAD™ software provides word descriptions integrated with the mathematical derivations and results, as well as the references used and discussed in this Exhibit.

The results of both sets of observation-calculation comparisons are presented in the results section, and the limitations, implications, and importance of the results are examined in the Discussion. These comparisons are also discussed in terms of the implied doses corresponding to the Geiger counter rate readings when it was switched from the count-rate scale used to determine beta ray fluence to the corresponding exposure rate scale.

# 2. BACKGROUND

## 2.1 **Importance of beta particle dosimetry in radiation protection**

In this thesis, we are interested in the response of the colorimetric dosimeters to a charged particle, the beta ray, entering its sensitive volume. As opposed to gamma radiation, which only delivers energy to a medium when it randomly interacts with an electron or nucleus of an atom in the medium, charged particles begin losing energy as soon as they enter the region as a result of the interactions of their electric fields with atomic charges even at some distance.

Ionizing charged particles that we commonly encounter in health physics (the profession of protection against harmful radiations) include beta rays, alpha particles and heavy atomic nuclei from cosmic particles. A beta particle is an electron or a positron emitted from the nucleus of a radioactive atom. They are much less massive and less charged than alpha particles and interact less intensely with atoms in the materials they pass through, which give them a longer range than alpha particles. Some energetic beta particles, such as those from P-32, can travel up to several meters in air or tens of mm into the skin, while low energy beta particles, such as those from tritium, are not capable of penetrating the dead layer of the skin. All beta emitters can pose a hazard if inhaled, ingested or absorbed into the body in sufficient quantities. In addition, energetic beta emitters are capable of presenting an external radiation hazard, especially to the skin.

Stopping power of beta particles is commonly separated into collision and radiative stopping power. The predominant interaction of beta particles in matter is with electrons through coulomb interaction. An important consideration in shielding beta particle radiation is the ability of beta particles to produce a secondary radiation called bremsstrahlung. The intensity of bremsstrahlung radiation is proportional to the energy of the beta particles and the atomic number of the material through which the betas are passing. Consequently, bremsstrahlung radiation is generally not a concern for lower energy beta emitters, and

especially for the low atomic number, Z, materials involved in this thesis. The fraction of the electron energy converted to bremsstrahlung in the X ray region is only ZE/800 where Z is the atomic number; E is the energy of the impinging electron in MeV. Most of the bremsstrahlung radiation produced in the uranium glaze is self-absorbed in this high Z material before it escapes to activate external detectors. Thus, the electrons that escape the uranium glaze can transfer only a fraction, less than about 1/800, of their energies into these very low energy x rays. It is known from many measurements that any skin doses from emissions of the uranium glaze are due primarily to the beta radiation emitted, as long as the elemental uranium has been chemically separated from those daughter (progeny) elements in the chain below uranium-234. The rates of energy loss per unit distance traveled in a medium by charged particle radiations are often given in units such as MeV per gram per square centimeter ($MeV\text{-}g^{-1}\text{-}cm^{-2}$).

Beta decay of a radionuclide results in three final products: the daughter nucleus, the electron or positron, and the neutrino or antineutrino. Conservation of momentum and energy do allow us to state that there will be a definite maximum kinetic energy given to the beta particle, occurring in the limit as the momentum and energy given to the neutrino approach zero. Emitted beta particles will have a continuous kinetic energy spectrum, ranging from zero to the maximal available energy, which depends on the parent and daughter nuclear states that participate in the decay. Differences in spectral shape are primarily responsible for variations in the shape of dose distributions from different beta emitters. Because of wide variation in spectral shape, the characterization of a beta-ray spectrum by its maximum energy or mean energy may not be adequate in some cases. Knowledge of beta-ray spectra is therefore important for the understanding of beta-ray penetration as an input to the calculation of dose distribution.

Beta ray hazards exist in the nuclear power industry, in the processing of radioactive ore, in medical, industrial and research applications of radioactive isotopes, around accelerators or from any possible accidental or deliberate release of radioactive substances. A threat from possible use of radioactivity dispersal devices by rogue nations and/or terrorist groups has also entailed planning for radiological emergency preparedness measures. Radioactivity dispersal devices (RDD), also known as "dirty bombs," are designed to use

explosive force to disperse the radioactive material over a large area. Such incidents may cause more psychological harm and panic to most of the public than actual harm or fatalities from radiation exposure, if members of the public cannot immediately know their actual exposures. Colorimetric dosimeters can be used in such incidents to alleviate most public concern about beta, as well as gamma, exposure, when worn to determine individual exposures.

In addition to real time readings, colorimetric dosimeters also read cumulative doses like any other passive dosimeter such as thermoluminescent dosimeters. Furthermore, the dose can be estimated immediately by the user, by examining its color. To support an effective response a physical dosimeter must accurately monitor dose in the range of 10 mGy (1 rad) to about 10 Gy (1,000 rad), instantly read cumulative dose, be affordable, portable, easy to use, and read dose with minimal training. The SIRAD family of dosimeters is especially unique in its importance for measuring skin or surface tissue doses because it is thin, small and unobtrusive, of low Z, and can be worn close to, or in contact with, skin. Other types of dosimeters having the same advantage of immediate observability of the dose to skin are larger, more expensive, and can not be so closely attached to skin. Additional advantages and the uses of the SIRAD family of dosimeters in peacetime or upon terrorist attack are in Brodsky (2010).

## 2.2 **Methods of measuring beta radiation dose**

Cylindrical GM counters with a circular end window, closed with thin mica circular walls, to minimize absorption of incident beta rays, have been used for the measurement of beta ray fluence from the early days of radioactivity measurements (Rossi et al 1949, pp 116-117). However, these counters were designed to determine electron (beta ray) fluence rates, not the deposited energies that could be used to determine tissue absorbed doses. The selection of current end-window types of GM counters for the detection, but not accurate dose-rate determination, of beta emitters of various energy spectra, and the estimation of surface beta radioactivity for radiation protection purposes, is presented by Johnson et al; 2001, pp. 318-319.

The primary concern in any personnel dosimetry system is to obtain measurements that can be converted to dose received by the human tissue of concern. Dosimetry results and instrument readings, therefore, generally require adjustments or built-in conversion factors to convert the air dose to tissue dose, or to provide "tissue equivalent" response. Ionization chambers with a thin entrance window are among the most widely used detectors for measuring beta-ray dose equivalent rates. The ideal design constitutes a thin, planar tissue equivalent chamber with tissue-equivalent window of about 0.07 mm thickness.

Thin window (2 mg/cm$^2$) GM counters are extensively used to measure the number of beta particles from surface contamination, with an extremely high sensitivity. Thin scintillation detectors and semiconductor counters have also been used in portable instruments to measure risks of beta emitters in surface contamination, but the dose estimates of these portable instruments from surface contamination can only be approximated. Film, thermoluminescent materials, and other solid state detection media have also been used, with different multiple filter designs, as personal dosimeters that can be worn on the clothing to discriminate between, and interpret doses from, x, gamma, and beta radiation (Cember 2001). However, such dosimeters are not applicable to precise beta dose-rate determinations. The dose response and the directional dose response, the variation of response with respect to direction 'Ω', are two important properties of a detector. The reading of an instrument H(d,α) at a certain tissue depth 'd' in a unidirectional(α) field of monoenergetic electrons will therefore vary with the direction of incident radiation. In the forward direction the variation of the quotient of H(d,α) and fluence is caused by the changes, with the angle of incidence, both of attenuation in a tissue layer of thickness 'd' and of backscattering. Beta radiation can be regarded as weakly penetrating radiation for which the directional dose equivalent H(d,Ω) should be used as an operational quantity for area monitoring, using a depth 'd' of 0.07 mm for the skin and 3 mm for the eye (Turner 2007).

For beta radiation, backscattering from the ICRU sphere is not significantly different from backscattering from a sufficiently thick plane slab. The standard instrument for precise beta ray dose rate determination is the extrapolation chamber for which the response, with respect to the dose equivalent H(d,Ω), is close to isodirectional; but it is not isotropic with respect to fluence. Dose equivalent and dose equivalent rates from beta radiation are often

difficult to measure because of their marked non-uniformity over the skin and their variations with depth. The best known measuring method that allows precise and absolute measurements of the beta dose rate of radionuclides within tissue equivalent phantoms makes use of the extrapolation chamber. However, the use of extrapolation chambers for precise measurements of beta ray doses from various distributions of beta emitters, within and on various media and body tissues, requires the availability of specially designed equipment (Loevinger 1956, Loevinger et al. 1956). This type of equipment is generally applied in a series of measurements of ionizations in air or other gas media, as two parallel plate electrodes at a constant collection voltage are slowly brought together, or as an ionization chamber mimics smaller and smaller volumes by sequential decreases in gas pressure. With such measurements, the ionization readings can be extrapolated to effectively zero ionization to obtain contributions from very low penetrating electrons (or x rays).

However, these precise laboratory extrapolation chambers, and their designs for particular geometries of tissue exposure, are not widely available for inexpensive, convenient use in accurately determining in field use the beta ray doses to persons whose skin might be contaminated with beta emitters or in contact with contaminated surfaces. NCRP has reported the difficulties in comparing laboratory measurements of beta dose even for small beta-emitting ("hot") particles of well-defined geometries (NCRP 1989).

## 2.3 **Methods of calculating beta dose from geometric distributions of beta emitters**

While estimating external beta-ray doses in monitoring practice has been routine for more than 50 years, the accuracy and reliability of field methods of beta dose determination have always been lagging behind those of gamma ray dosimetry. This can be attributed partly to the usually smaller risk to personnel from beta than gamma radiation. It can also be attributed to the difficulties of determining the large variations of dose over short distances in tissue, and the need to measure doses in very thin layers at the depths of basal cells from the surface of skin (conservatively estimated as at 70 micron or 7 mg/cm$^2$ depth in radiation protection standards). These difficulties of measuring beta doses and dose rates with finite

size detectors in practice are even more accentuated in the precise determination of beta doses with laboratory instruments that must be designed and set up for very specific geometrical configurations in order to obtain accurate dose determinations at specific tissue sites.

Therefore, the primary determinations in this thesis of beta doses for comparison to those visually observed on the SIRAD dosimeters must be made by calculations, based on estimates of beta ray fluence and energy spectra determined from the count rates of end-window detectors. A brief summary of the principles of beta dose calculation described in the radiological physics literature is presented in the following paragraphs.

The most common assumption for calculating dose distribution from localized beta-particle has been the use of a point source distribution. The problem of determining the absorbed dose around a localized beta-particle source in tissue can be separated into two steps. First, the distribution of dose around a (hypothetical) point source of beta-particles in tissue is determined from laboratory measurements. Second, the dose distribution in and around a geometrically-defined beta-particle distribution in tissue is calculated by suitable summation of the elementary point source distributions.

The nature of the beta-particle point source distribution is rather complicated. The absorption and scattering of electrons is a function of energy, so that the average electron paths in absorbing media can only be found by rather elaborate theoretical computations. The determination of the spatial distribution of absorbed dose from beta rays for a variety of boundary conditions has been approached using both experimental measurements and theoretical calculations. The advent of high-speed computers has made it practical to develop calculations that treat the transport processes with an increasingly high degree of accuracy: thus, such computer calculations provide results that are now often considered as reliable as measurements.

Different analytical methods were designed for calculation of dose distribution. The beta dose distribution about a unit point source of radioisotope of interest is referred to as the beta dose point kernel. The original point source dose function was proposed by Loevinger

(Loevinger 1956). On the basis of his measurements, Loevinger proposed an empirical function describing the dose distributions around a hypothetical point source for different beta emitters.

$$J(x) = \frac{B}{(\rho\nu x)^2}\left\{c\left[1 - \frac{\rho\nu x}{c}\exp\left(1 - \frac{\rho\nu x}{c}\right)\right] + \rho\nu x\, exp(1 - \rho\nu x)\right\} \quad \text{....Eq. 1}$$

with the quantity between square brackets ≡ 0 for ρνx ≥ c. In this expression: J(x) is the absorbed-dose rate per unit activity (in Gray per megaBecquerels per hour) at a distance x (in centimeters) from the point-source; ρ is the apparent absorption coefficient (in square centimeters per gram); ν is the density of the homogeneous medium (in grams per cubic centimeter); c is a dimensionless parameter, which gives the value between square brackets at x = 0 and is also the value of ρνx at which this term between square brackets becomes and remains zero and B is a normalizing constant. Loevinger's pioneering work has served its purpose for a long time in the dosimetry of beta emitters used in clinical applications (ICRU 2004).

Calculation of skin doses resulting from contaminants on the skin or on protective clothing worn over the skin are frequently performed at many facilities that use, or generate, unsealed radioactive materials. Several methods are available for performing these calculations, including the use of formulas such as those developed by Loevinger as well as various point and plane source tabulations. These tabulations, however, frequently involve considerable effort to integrate the point kernels over the source volume of interest, and in such cases, a computer code that performs these manipulations provides considerable simplification.

VARSKIN is a code developed in government laboratories, and is designed to integrate beta dose based on the point kernel developed by Berger (Berger et al 1959, Berger 1971). This code is used in this work with permission from the Oak Ridge National Laboratory. The code has been in use for many years, and has become an industry standard for this type of calculation. It is used by the U.S. Nuclear Regulatory Commission (NRC) for evaluating the dose to contaminated skin and comparing it to regulatory limits. The most

recent version of the code, VARSKIN-3, was written to operate in a Windows environment using a graphical user interface (Durham et al. 1992; Shapiro 2002).

Mathematically, Berger's point kernel is written as:

$$B(r) = \frac{kE_{\beta}YF_{\beta}\left(\frac{r_1}{X_{99}}\right)}{\left(\pi\rho r^2 X_{99}\right)} \qquad \text{.....Eq. 2}$$

Where B(r) = the dose rate at a point at distance r from a source point, r = the distance between a source point and the dose point, k= a unit conversion factor, $E_{\beta=}$ the average beta energy for the radionuclide, Y= the beta yield per disintegration, $F_{\beta}$ ($r_1/X_{99}$) = the scaled absorbed dose distribution, $r_1$ = the modified path length between a source and the dose point, ρ= the density of the irradiated medium (assumed to be unity for tissue). The $X_{99}$ distance is defined as the radius of a sphere of water surrounding a point source of the beta radiation in which 99 percent of the beta energy is deposited. VARSKIN 3 calculates $F_{\beta}$ ($r_1/X_{99}$) for a selected radionuclide when the radionuclide is added to the library.

Comparison of VARSKIN 3 code beta skin dose calculation results for beta energy in the range of 0.3MeV - 2.3MeV were done against Monte Carlo N-Particle transport code (MCNP) results by Sherbini et al. (2008). The results showed excellent agreement within a few percent for point and disk geometry, and within 20 percent for other sources with the exception of few cases.

## 2.4 **Colorimetric Dosimeters**

The concept of radiation dosimetry arose shortly after the discovery of natural radioactivity. Ionizing radiations were soon observed to cause fluorescence of certain substances. The first dosimeters depended upon the fluorescence of the platinocyanide of barium in the presence of gamma radiation (George et al. 1951). Different methods and types of dosimeters that are also specific to the type of radiation have been developed through time. Quantifying the level of ionization of atoms and molecules of exposed substance such as air, water, or tissue-equivalent substances, in measuring instruments was the main physical process involved initially in the fundamental dosimetry of ionizing radiation. In chemical

dosimetry, the dose is determined by measuring the chemical yield in the medium of the dosimeter due to irradiation.

Colorimetric dosimeters are chemical dosimeters that are used to measure absorbed dose by observing the color change that is dependent on the extent of a chemical reaction caused by the ionizing radiation to be measured. For emergency responders and public use, the needs are qualities such as: instant reading of dose; minimal training to read doses and understand the corresponding levels of harm indicated by color changes; the capability of measuring doses in the ranges of interest; affordability; and always ready availability for use. Historically, colorimetric dosimeters have been limited to high dose measurements; Examples include the liquid-phase US Army Tactical Dosimeter that measures dose in the range of 0.5 to 4.5 Gy, and the Fricke dosimeter, which measures doses above 10 Gy. Recently-developed colorimetric dosimeters such as SIRAD (by JP Laboratories Inc.) which have been tested by the department of Homeland Security and approved for distribution to responders, are designed to measure lower as well as higher doses, which makes such dosimeters useful in a wider range of situations for emergency responders.

Self-indicating Instant Radiation Alert Dosimeters (SIRAD™) are colorimetric dosimeters developed by Dr Gordhan Patel at JP Laboratories Inc. In addition to the investments of Dr. Patel, these dosimeters have been developed with funds from a number of Federal agencies, beginning with research of the Navy Department (Riel et al. 2006). These dosimeters have been tested by the U.S. Department of Homeland Security (DHS) through field deployment, laboratory irradiation, and visual readout; the overall outcome demonstrated an acceptable performance for homeland security mission needs (Klemic et al. 2007; Buddemeier 2007). Based on the test results, there remains only a decision to be made by DHS policy makers as to whether SIRAD needs to be included in their standards for emergency responders and the public in the United States (Brodsky 2010). These dosimeters are already being distributed in large quantities in Japan, since the Fukushima reactors released radioactive effluents after the recent tsunami.

The SIRAD family of dosimeters comes in two different forms: a RADSticker, which is a peel-and-stick type, postage-stamp-size, thin-plastic dosimeter, with a dose reading range

of 25-1000 rad, and a RADTriage-FIT credit-card-size dosimeter with increased sensitivity for low-energy radiations, which can be read in the range between 1-10,000 mSv (or with a conversion factor of 1 rad (or rem) = 10 mSv). On the side of the active element is a **FIT™** indicator (false indication test), which helps to determine tamper or color changes caused by prolonged exposure to direct sunlight or UV. In such cases the cover film on the FIT can be pealed off and any color difference between the exposed active element and the uncovered element shows a tamper on the dosimeter.

When exposed to radiation, these dosimeters develop color instantly and the color intensifies with dose. The different colors on either side of the sensor are developed by Dr. Patel using a 100 KVP cabinet X-ray source. A calibrated table of values for specific dose selection helps to choose the appropriate dose of X-ray or gamma radiation generating a specific color. The X-ray source exposure times are used to deliver the amounts of dose needed to calibrate the corresponding color changes of the square areas beside the sensitive center strip; these squares are fixed in color and labeled according to the corresponding dose to be read on the center strip. For higher dose colors multiple applications are required, shielding the rest of the chemical dosimeter with thick lead plate. The colored squares for comparison are arranged so that a wearer of the dosimeter can easily see whether the color of the center strip is darker than all the squares up to 25 rad (or 0.25 Sv on those RADTriage cards that use special SI units), which are placed beside the center strip. In this design, a wearer with very limited training can at least tell whether he is receiving more or less than 25 rad by observing whether the center strip is darker or lighter than the squares on the side of the strip representing up to 25 rad (or even higher doses for the squares lined up on the other side of the sensitive center strip). See the dosimeters in Figure 1 and the sequentially exposed dosimeters in Figure 8.

### 2.5 **Uranium-glazed plates as sources of beta radiation**

The sources of beta radiation in this thesis are uranium glazed tableware. Starting in the early 1930s, naturally-occurring radioactive materials found their way into the manufacturing of glassware, ceramics and granite countertops. Uranium oxide and sodium uranite were used to produce the glaze; and the concentrations of these glazes were estimated

to be 10 to 20% by weight (Piesch et al 1986). The hazard from bare skin contact with uranium containing tableware is expected to be mainly from uranium-238 daughters' beta emissions. The only gamma activity is from $^{214}$Po and when measured at surface of orange ceramic saucer plates it was found to be in the order of one-fifth of the magnitude of the beta emission (Buckley et al 1980), and thus produce a much smaller fraction of the dose. The fraction of the beta dose to skin from this gamma emission is far below one-fifth of the beta dose to skin. Although the uranium glaze emits gamma, alpha and beta particles, both gamma and alpha emissions are very weak and the beta particles are considered responsible for the bulk of radiation exposure from glazed ceramic plates.

In radiation protection beta-ray dosimetry provides dose information that will help in keeping any harmful effects of beta-rays within acceptable limits. In the event of serious over-exposures, measured estimates of the dose will assist medical treatment and prognosis. In routine industrial or research operations with beta-emitting radionuclides, the external dose to betas is protected against by shielding available; otherwise, dosimeters worn as rings on the fingers or personal monitoring badges provide monitoring of the dose using several filters to discriminate between beta and gamma exposure rates. Beta emitters rarely pose an internal hazard in routine operations; internal beta exposures in the history of operations with radioactive material have been shown to be minimal. External protection from beta radiation is usually a simple matter of interposing a thin layer of low-Z material between source and tissue.

In most practical situations, because of a strong attenuation by air and clothing, beta rays with maximum energies below 200KeV provide a hazard only when the source is directly on the skin. An external hazard is therefore only likely when a high concentration (above about 0.1 microcuries per square centimeter) of any beta-emitting contaminant is allowed to remain on the skin for prolonged periods of time. This is not likely to occur under required practices for handling and monitoring operations with licensed radioactive materials.

Under most beta exposure circumstances, deterministic effects in the skin are considered to be of more concern than stochastic effects. In some cases, beta-ray doses from

unshielded sources may be more than 50 times larger than gamma-ray doses from the same source (ICRU Report 56 1997). An extreme example of such a situation occurred in the Chernobyl accident, where a number of workers received beta-ray doses that contributed substantially to their deaths (IAEA 1986).

### 2.6 **Unattenuated Beta energy spectra of nuclides from Uranium glaze**

Among the decay products of $^{238}U$, close to a dozen of the progenies undergo beta decay. Considering $^{222}Rn$ which leaves the surface as gas, only the daughters before Radon contribute to the beta surface dose from a glazed ceramic. The beta activity of uranium metal therefore comes primarily from $^{234}Th$, $^{234m}Pa$ and $^{234}Pa$ (Thomas et al 1994). The average and maximum energy of the respective beta spectrums are $^{234}Th$ = 43.5KeV (193KeV-max), $^{234}Pa$ = 214KeV (530KeV-max), and $^{234m}Pa$ = 819KeV (2.29MeV-max). The beta energies of thorium are very low; both the GM counter and SIRAD dosimeters have very low sensitivities to such energies. The calculations therefore consider only isotopes of protactinium. A partial decay chain of uranium and beta spectra of protactinium isotopes are shown in Figure 2.

## 3. METHODS USED IN THIS THESIS

### 3.1 **Dose measurements**

The accurate and expensive extrapolation-chamber types of measuring equipment described in section 2.2 were not available for this thesis. Repeated attempts were made to obtain assistance from the appropriate experts at the National Institute of Standards and Technology (NIST), but their intense budgetary efforts at the time this work was begun did not allow them to respond. Without considerable funding, neither were secondary beta ray sources that provide calibrated beta dose rates available for this study. Therefore, it was decided to use count-rate instrument measurements to characterize the fluence and energy distribution of beta radiation emitted from uranium glazes, and calculate by two independent methods the doses from the uranium glazes over specific time periods, for SIRAD dosimeters

in close contact with these GM and NaI count rate instruments. In this way, independent estimates of doses received by the SIRAD dosimeters, as obtained by two fundamental calculations, were made available for comparison with indicated doses as estimated by color changes on the (x-ray-calibrated) SIRAD dosimeters. These comparisons were then used to conclude whether the dosimeters were capable of providing at least approximate estimates of the received beta doses.

Therefore, the only measurements made for this study were GM counter and thin-window, 1-mm-thick, NaI detector count rates to estimate the emission rates of beta particles from the uranium glaze samples used to expose the SIRAD dosimeters. The GM counter used was a RADIATION ALERT ® INSPECTOR™ model[1]. The scintillation detector used was a thin-window, 1-inch diameter and 1-mm thick NaI detector, coupled to a separate counter unit to read the number of counts per minute.

The GM counter measurements were primarily used to estimate the beta-ray fluence rates, but were confirmed to be consistent by sample measurements with the NaI detector. The RADIATION ALERT GM counter used has a 1.75 inch diameter pancake mica window. Attenuation of the beta fluence by the window, over the vast majority of the emitted beta energy spectrum determined by absorption measurements, was negligible for the accuracy requirements of this study. The GM counter measurements of the beta count-rates could also be compared with the mR per hour readings when the switch of the instrument was changed to read exposure rates corresponding to count rates. In this way, another independent, although approximate, estimate could be obtained of the exposure rate that would be obtained in a gamma ray field giving the corresponding count-rate. The corresponding gamma doses indicated are easily calculated from the indicated exposure rates, giving another independent set of doses to use in approximate comparisons with the dosimeter color changes. These comparisons are in addition to those calculated from the count-rate measurements, but are also important because those are the methods by which wearers will interpret their exposure and/or absorbed doses, for comparison with risk levels. Two different uranium glazed plates were used as sources of radiation for the RADSticker and RADTriage.

[1] Manufactured by S.E. International, Inc., P.O. Box 39, 436 Farm Road, Summertown, TN 38483-0039 USA.

## 3.2 **Methods of calculating beta doses from uranium glazed plates**

Two separate approaches were used to calculate the beta doses at the points on the surfaces of the plates where the centers of dosimeters were exposed. The first approach used the VARSKIN 3 code (Durham et al. 1992), which was described in section 2.3. The second calculation method, as an independent check on the use of VARSKIN in this thesis, is based on an algorithm that is modified to incorporate an additional integration of beta doses over incident angles and stopping powers as functions of energy. This second method, presented in Exhibit A, was developed for a circular plane geometry beta radiation source of protactinium-234m, by extending an algorithm for determining gamma ray dose rates above a plane circular source of gamma-emitting photons (Brodsky et al 2004). The detailed assumptions and formula for this model, together with results, are included in Exhibit A. A brief description of the code and the parameters entered into the VARSKIN code for purposes of this thesis, and the rationale for using these parameters, are described in following paragraphs.

VARSKIN 3 has a single data entry page which allows the user to select the radionuclide, the model geometry under consideration (out of the six predefined source configurations: point, disk, cylinder, sphere, slab and syringe) and an option to add the required dimension, exposure time and exposure or decay rate. The source radionuclide is selected from a library of radionuclides; when a radionuclide is selected, the code extracts the beta spectrum of the particular radionuclide from ICRP-38 (ICRP 1983) data located in one of the directories of the code's file. The radionuclide library file contains all known electrons and any photon with energies that would contribute to effective skin doses, but it requires the user to enter the nuclide and all existing radioactive progeny expected to be involved in the calculation.

The code models the point source as a cylinder with a thickness of 1 μm, a radius of 1 μm, and a density of 0.001g/cm$^3$. The disk source is recommended for modeling liquid skin contamination events and it is modelled as a cylinder with thickness of 1 μm, and a density of 0.001g/cm$^3$, whereas the surface area will have the dimension of the radius entered. The cylinder source geometry assumes that the source is surrounded but that the entire bottom of the cylinder is in contact with skin or cover material.

The code includes a backscattering correction for all three dimensional sources with dimensions from the skin smaller than the range of the beta particle. The range is equated to the $X_{99}$ distance mentioned in Berger's Kernel (shown in Equation 2) above, which is the radius of a sphere of water surrounding a point source of beta radiation in which 99 percent of the beta energy is deposited. VARSKIN-3 calculates the beta dose rate by performing a numerical integration of the Berger point kernel. The integration is performed by choosing 60 dose points at which the dose rate is to be calculated beginning at the source centerline and proceeding radially outward from centerline at the skin level depth. Since the source is symmetric, dose points represent concentric isodose circles that describe the radial dose rate profile at a given depth in skin. For each dose point, integration is performed over the area of the disk-shaped source at a given height in the source for eight consecutive height points as shown in the equation bellow.

$$\dot{D}(d) = \int_0^{2\pi} \int_0^{R} \int_0^{Thickness} S_v \, B(r', \theta, Z) r' \, dZ \, dr' \, d\theta \qquad \text{---------- Eq 3}$$

Another eight radial points located at equiangular points are taken, and then for these eight height circular planes and each of these eight circular points, the dose rate is calculated. This process, known as the Newton-Cotes eight-panel quadratic routine, provides a fast and accurate method of numerical integration of complex functions such as the Berger Kernel (Durham 2006). The dose rate at each of 60 dose points are then calculated using a similar procedure and averaged over an area in the skin. When modeling the three-dimensional source attenuation due to the presence of the source material and attenuation due to geometry ($1/r^2$) are addressed. Finally, the output window of the code displays the calculated result in three distinct quadrants; the results show contributions from each individual radionuclide, the combined results from all radionuclides, and source input data.

When using the VARSKIN-3 code, certain assumptions pertaining to the number of beta sources expected as daughters of uranium decay and the geometry of the source were considered. Assumptions included in the calculation are:

- The area of the source is assumed to be the same as the area of the GM counter window. The GM counter has an effective window diameter of 1.75 inch and an area of 2.41 square inch is then considered as area of source.

- The skin area was considered taken to be the same as the size of the source which is again 2.41 square inch.
- The skin thickness was taken to be the thickness of the amber film which covers the radiosensitive chemical on SIRAD. The thickness of the film is 50 micron and this was then taken to be the skin thickness.
- The uranium glaze source is considered as a disk source which is similar to a plane source considered in other models and the default source density and source thickness of 1 mg/cm$^3$ and 1 micron respectively were considered in the calculation.
- Due to a raised ring pattern on the saucer surface it was not possible to bring the GM counter windows in contact with the saucer. To compensate for the distance an air gap of 0.2cm was also considered.
- Based on the efficiency of the GM counter to the energies of the isotopes under consideration that is close to 50%, the number counts obtained were considered to be half the actual counts the SIRAD dosimeter will see while in contact with the surface.
- The total count was also divided among the individual progeny of uranium based on the sensitivity of the GM to the specific energy of the individual progeny. To this effect when only the two protactinium isotopes are considered the count is divided equally where as when $^{234}$Pa, $^{234m}$Pa and $^{234}$Th are considered 2/5 of the total count is assigned to each protactinium isotope and the remaining 1/5 is assumed to be contribution from thorium.

Finally the actual exposure time period of 110 days with an average GM count of 22,257 counts per minute (CPM) were used for the RADSticker, and 55 days with an average GM count of 40,670 CPM were used for the RADTriage card.

### 3.3 Absorption measurements to characterize the emitted spectrum from uranium glazed plates :

To better characterize the beta spectrum from the glaze, an estimate was made from its maximum range and shape as estimated from beta attenuation measurements. Beta attenuation measurements used count rates from the GM counter and the 1-mm-thick NaI scintillation detector as thicknesses were increased of known-density paper; the data collected are shown in Table 2. The simulated absorption spectra in the graphs shown in

figures 6a and 6b indicate a beta ray maximum range close to 1100 mg/cm$^2$, which indicates from Figure 7, that the maximum energy of the beta spectrum is about 2.2 MeV, similar to that from $^{234m}$Pa. Also, the absorption curves show the range of beta rays in low Z material. From the rule of thumb that the range in g/cm$^2$ is about half the maximum beta energy in MeV (Voss 2010), the absorption experiments therefore indicate a maximum beta energy of about 2.2MeV, consistent with the maximum energy of the metastable Protactinium $^{243m}$Pa.

### 3.4 Statistical tests on the uniformity of uranium glaze

Uniformity of the irradiation at the surface of the beta source was tested using by variance analysis of the CPM and mR/Hr data taken at different points of the ceramic glaze. The F-test is a method of statistical variance analysis that is used to assess whether the measured values of a quantitative variable within several pre-defined groups differ from each other. It is used in this case to assess whether any of the measured values is on average superior or inferior to the others versus the null hypothesis that all four yield the same mean dose. This was done by taking data of count rate and dose measurements from one of the saucers by placing the meter at four different positions. The measurement points were marked as A, B, C and D and the measured values are listed in table 1; the statistical analysis of these values is shown in Table 2. The calculated F-test values show that the differences in sample standard deviations at different points on the glazed plates can be claimed with 95% confidence to be due to random error. This shows that the measured values at any one of the four positions are equally valid representations of beta surface rate emissions for use in the dose calculations.

### 3.5 Interpretation of darkening of SIRAD dosimeters in terms of absorbed dose

During exposure a radiation-induced polymerization of the diacetyelenes in the sensing strip starts instant color change that intensifies to dark blue with increases in dose, but is independent of dose rate. The color change can also be caused by excess heat, exposure to ultraviolet, and other disturbances, and thus must be worn or kept under conditions

specified by the manufacturer. However, other dosimeters have similar conditions. Each RADTriage card dosimeter has the "FIT" indicator described in section 2.4 above that alerts the user to any false indications due to exposures other than ionizing radiation.

The SIRAD dosimeter thicknesses are also designed to reduce any possible attenuation of radiation entering the sensor from back or front. Reading is done by the wearer with a naked eye and has an uncertainty of 20% for the RADTriage and 25% for the RADSticker. Although intended for visual reading the dose may be read to about 10% uncertainty if optical density is measured using a spectrophotometry. For this thesis, visual readings of the color changes of the RADTriage and RADSticker were taken, and for confirmation, Dr. Patel and an experienced member of his staff were consulted and their evaluations were accepted as best.

# 4. RESULTS

Based on the visual reading of the color change on each type of colorimetric dosimeter, the readings from the RADSticker and RADTriage were estimated by eye and recorded to be within the range of 10-15 rad and 350-400mSv (35-40rad), respectively. Similarly, for the RADSTicker, calculations based on VARSKIN (using the variables and assumptions used in section 3.2 above), and the direct integrals inExhibit A, resulted in doses of 24 rad and 21 rad, respectively. For the RADTriage, a VARSKIN calculation was the only calculation method used and the result was found to be 21.9 rad. These results are summarized in Table 1a & 1b bellow. A picture of both SIRAD dosimeters after exposure is shown in Figure 4.

The approach and results of the direct integration method of Dr Brodsky are in Exhibit A. It is noted in Exhibit A that the estimate of 21 rad from the triple integral for a glaze- to-GM entrance distance of 3 mm was believed to be exactly consistent with the dose of 21 rad calculated from the rules of thumb in Shapiro (2002). However, this could be fortuitous, as discussed in the next section.

The dose of 21 rad calculated for the RADSticker may seem a bit high compared to the reading of 10-15 rad estimated by eye by the experienced technician at JP Laboratories. However, the calculated dose of 21 rad, which was initially believed confirmed by the

methods in Shapiro's book, might well be somewhat high, for reasons given in the Discussion. Further differences in the readings and the calculated results of SIRAD dosimeters can be attributed to a number of sources of error, which are considered in the discussion below.

**Table 1a.** Results of color change readings for RADSticker and RADTriage vs. calculated doses

| Type of SIRAD | Isotopes Considered | Exposure time (days) | Reading from SIRAD color change (rad) | Calculated dose result (rad) |
|---|---|---|---|---|
| RADSticker | $^{234}$Pa, $^{234m}$Pa | 110 | 10-15 | 28.1 |
| | $^{234}$Pa, $^{234m}$Pa, $^{234}$Th | | | 24.0 |
| RADTriage | $^{234}$Pa, $^{234m}$Pa | 55 | 35-40 | 25.6 |
| | $^{234}$Pa, $^{234m}$Pa, $^{234}$Th | | | 21.9 |

**Table 1b)** Dr Brodsky's calculation on RADSticker using method attached in exhibit

| Radius of Beta source(cm) | Air gap(cm) | Exposure time in days | Decay rate (CPM) | Reading from SIRAD color change (rad) | Calculated dose result (rad) |
|---|---|---|---|---|---|
| 2.0 | 0.2 | 42 | 32000 | 10-15 | 17.353 |
| 2.38 | 0.3 | 110 | 32000 | | 25.276 |
| 2.38 | 0.3 | 110 | 32000 | | 21.137 |

## 5. DISCUSSION

The lowest readable dose on SIRAD dosimeter scale sensitivity range can be close to half the annual occupational dose limit. Therefore, these SIRAD dosimeters, which have been designed for emergency use would not be considered sufficiently accurate for routine recording of occupational exposures, where it is of interest to continually follow and limit the accumulation of smaller radiation exposures. However, they can be used as backup dosimeters to warn wearers when they are approaching a 5 rad annual limit for gamma dose, or a 50 rad limit of skin dose, and verify whether or not such a limit has been exceeded when

a worker has lost his badge during an operation that could possibly cause high exposures. A SIRAD dosimeter in the wallet, for example, would thus be a back up for the personal monitoring. In most such situations, it would not be likely that the visual readings of color change or darkness would be in the exact range where the decision of exceeding, or not exceeding, a dose limit would be confounded by the errors in observed readings.

Uncertainties in the measurement of the count rate with the GM counter and NaI are the first uncertainties that propagate into the methods of calculation. Counts taken by either instrument are sufficiently large, as presented in Table 2, that counting errors are not a major cause of error in the calculations of this thesis. Poisson errors of counting are negligible compared to the other compound uncertainties in this type of observational experiment.

The F-test results discussed in the precious sections indicate that counts taken from different section of the glaze demonstrate that the glaze is rather uniform for our purposes. The main error in estimating the dose indicated by the SIRAD dosimeters from the surface of the glazed plates isevidently be the uncertainty in human judgment of the darkness of the exposed center strip of the SIRAD dosimeter compared to the indicated darknesses in the adjacent squares, which are labeled at different doses. As indicated earlier, Dr. Patel has estimated these uncertainties as on the order of 20 percent; it is assumed that this uncertainty approximates a standard deviation in a single observational estimate over the dose range up to about 100 rad (1 gray or 1,000 mSv) (see Figure 8).

Another possible cause of error might be the size of the exposed area considered. The count rate considered in the calculation is taken based on the dimension of the counter window, whereas the radiation detector covers a smaller portion of the area of the SIRAD dosimeter. This assumption, assuming two-pi geometry, or a fluence of electrons into the counter windows that is exactly one-half of that emitted from the same area of the glaze as the area of the counter window, might well cause an overestimate of dose by the calculations. Although the initial calculations of Exhibit A, using a distance of 3 mm between the surface of glaze and the entrance to the GM tube, gave good agreement with calculations using the rules of thumb developed in Shapiro (2002), there is evidence in Exhibit A that, at closer distances, it might also be necessary to include a consideration of the attenuation of electrons by skin tissues within the very thin 0.07 mm “dead” layer of skin, when calculating doses to

cells behind the dead layer from beta particle incident at wide angles. This calculation would then require an integration over only the energy range of the beta spectrum that could reach the target cells from each set of wide angles defined by the differential areas at a given radius. This can be done, because the functions for the spectra and the associated mass stopping powers vs. energy of electrons reaching the target cells are defined in Exhibit A.

## 6. CONCLUSIONS

This work shows that the SIRAD dosimeters can be used for beta measurement within a range of uncertainty, but that the uncertainty might well not preclude the value of possible indications of high beta doses under emergency conditions. Any skin dose from beta radiation that would cause permanent skin damage, or result over a long term in skin cancer, would certainly be detected by color changes well before such high doses would be received, certainly in time for effective skin decontamination. Discrimination between gamma and beta exposures, would of course require the use of at least two dosimeters, one of which must be shielded from beta radiation exposure.

Nevertheless, due to the limited number SIRAD measurements it is difficult to conclude that these dosimeters are suitable for measuring beta dose as accurately as some of the other, more-expensive, instruments that might be available for field use by responders or scientists who might later arrive on the scene hours or days after an attack or exposure. Reading accuracy could be improved if a spectrophotometer is used as mentioned above.

However for practical use in an emergency situation, the uncertainty should be taken into account and the dosimeter should be used to estimate the doses received to provide timely warning of the approach of serious exposures. Due to the limited range of beta particles, the external hazard is mostly limited to cases where the radioactive source is in contact with the skin. Therefore, SIRAD dosimeters distributed to the public would be important in situations where the possibility of such skin contamination is likely from RDD and nuclear industry accidents. An early indication to the wearer of changes in darkness of the center strip of a SIRAD dosimeter would serve notice to the wearer of the need for thorough washing and decontamination.

Another important conclusion of this investigation is that when uranium glaze dishes are available, as they often are to antique collectors, they can serve as check sources, or approximate calibration sources, for instruments or dosimeters that measure beta radiation, and also as effective check sources for any open window detector that measures any kind of ionizing radiation. This is important because the availability of calibration sources for civil defense purposes, and of licenses for their possession, was unfortunately curtailed when Federal assistance to the States for radiological preparedness was discontinued in the 1990s (Brodsky 2011). This lack of calibration sources for responders has been one of the discouragements in re-building radiological defense preparations for homeland security.

# TABLES

**Table 2.** Data for testing uniformity of Uranium glaze:

Measurement point A

| | | | | | | | | | | |
|---|---|---|---|---|---|---|---|---|---|---|
| CPM (1000) | 21.72 | 21.69 | 21.56 | 22.89 | 22.62 | 22.71 | 23.3 | 22.12 | 22.91 | 21.08 |
| mR/Hr | 6.76 | 6.87 | 7.47 | 7.38 | 7.29 | 7.07 | 7.18 | 7.04 | 7.13 | 7.19 |

Measurement point B.

| | | | | | | | | | | |
|---|---|---|---|---|---|---|---|---|---|---|
| CPM (1000) | 22.38 | 23.12 | 22.41 | 22.17 | 22.49 | 22.86 | 24.1 | 21.75 | 21.97 | 22.49 |
| mR/Hr | 7.43 | 6.85 | 7.32 | 7.24 | 6.87 | 6.93 | 7.62 | 7.03 | 7.69 | 7.00 |

Measurement Point C

| | | | | | | | | | | |
|---|---|---|---|---|---|---|---|---|---|---|
| CPM (1000) | 22.23 | 22.25 | 21.62 | 23.06 | 22.67 | 22.34 | 21.14 | 22.69 | 22.89 | 21.01 |
| mR/Hr | 7.11 | 7.06 | 6.87 | 7.13 | 7.19 | 6.97 | 7.10 | 6.77 | 6.77 | 7.10 |

Measurement Point D.

| | | | | | | | | | | |
|---|---|---|---|---|---|---|---|---|---|---|
| CPM(1000) | 22.32 | 22.08 | 20.82 | 22.04 | 21.75 | 22.17 | 21.71 | 23.26 | 22.58 | 21.36 |
| mR/Hr | 6.79 | 6.82 | 7.17 | 7.091 | 7.5 | 6.98 | 6.98 | 7.11 | 6.98 | 7.10 |

**Table 3:** Absorption data on beta intensities by layers of paper, for both GM and NaI thin window detectors

a) Measured values using GM counter

| Density in mg/cm^2 | Average mR/Hr | Average CPM | LN(CPM) |
|---|---|---|---|
| 97.3 | 4.30 | 14074 | 9.55 |
| 194.6 | 2.79 | 8860.4 | 9.09 |
| 291.9 | 1.70 | 5438 | 8.60 |
| 389.2 | 0.99 | 3400.2 | 8.13 |
| 486.5 | 0.57 | 1854.2 | 7.53 |
| 583.8 | 0.34 | 1033.2 | 6.94 |
| 681.1 | 0.17 | 524.8 | 6.26 |
| 778.4 | 0.08 | 284 | 5.65 |
| 875.7 | 0.05 | 163 | 5.09 |
| 992.5 | 0.03 | 99.4 | 4.60 |

b) Measured values using NaI detector

| Density in mg/cm^2 | Counts in 8/10 of a minute | LN of counts |
|---|---|---|
| 97.3 | 2988 | 8.00 |
| 194.6 | 2379 | 7.77 |
| 291.9 | 1899 | 7.55 |
| 389.2 | 1625 | 7.39 |
| 486.5 | 1429 | 7.26 |
| 583.8 | 1306 | 7.17 |
| 681.1 | 1259 | 7.14 |
| 778.4 | 1130 | 7.03 |
| 875.7 | 1127 | 7.03 |
| 992.5 | 1042 | 6.95 |

**Table 4.** Statistical variance analysis values based on table 1 above

| | CPM (X1000) | | | | Dose rate In mR/Hr | | | |
|---|---|---|---|---|---|---|---|---|
| | AVG | VAR | STDEV | F-Test | AVG | VAR | STDEV | F-Test |
| A | 22.26 | 0.528 | 0.726 | | 7.137 | 0.047 | 0.218 | |
| B | 22.57 | 0.444 | 0.666 | 1.189 | 7.196 | 0.095 | 0.308 | 1.996 |
| C | 22.19 | 0.508 | 0.713 | | 7.006 | 0.023 | 0.153 | |
| D | 22.01 | 0.446 | 0.668 | 1.141 | 7.052 | 0.04 | 0.2 | 1.711 |

**Table 5:** Beta spectrum data used in calculation: The beta decay data bellow which is used in the VARSKIN code for the two $^{238}U$ progenies ($^{234}Pa$, $^{234m}Pa$) are generated from ICRP 38 and a copy is accessible through the link: http://www.doseinfo-radar.com/radardecay.html

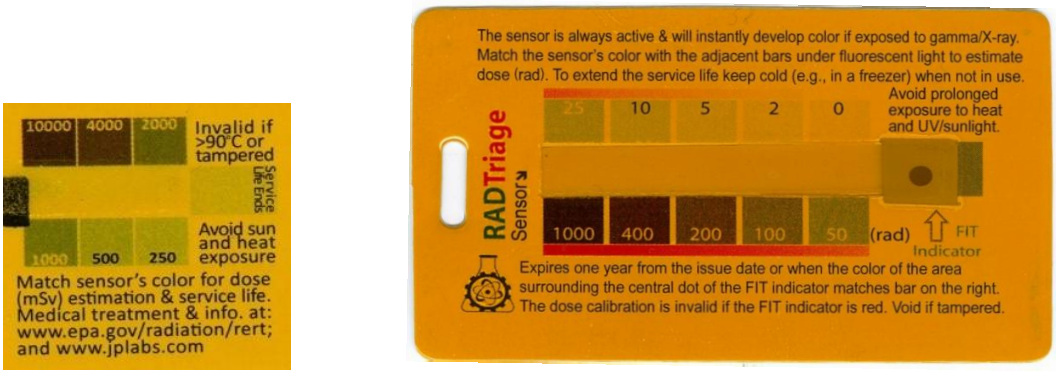
$^{234}Pa$ Beta Decay spectrum energies

| # beta particle /transition | Energy (MeV) Average |
|---|---|
| 2.14E-01 | 0.03 |
| 1.87E-01 | 0.09 |
| 1.58E-01 | 0.16 |
| 1.26E-01 | 0.22 |
| 9.36E-02 | 0.28 |
| 6.46E-02 | 0.35 |
| 4.20E-02 | 0.41 |
| 2.85E-02 | 0.47 |
| 2.16E-02 | 0.54 |
| 1.68E-02 | 0.60 |
| 1.33E-02 | 0.66 |
| 1.08E-02 | 0.72 |
| 8.52E-03 | 0.79 |
| 6.32E-03 | 0.85 |
| 4.33E-03 | 0.91 |
| 2.65E-03 | 0.96 |
| 1.39E-03 | 1.04 |
| 5.57E-04 | 1.10 |
| 1.53E-04 | 1.16 |
| 1.59E-05 | 1.23 |

$^{234m}Pa$ Beta Decay spectrum energies

| # beta particle/ transition | Energy (MeV) Average |
|---|---|
| 5.64E-02 | 0.06 |
| 6.53E-02 | 0.17 |
| 7.23E-02 | 0.29 |
| 7.74E-02 | 0.40 |
| 8.05E-02 | 0.51 |
| 8.15E-02 | 0.63 |
| 8.06E-02 | 0.74 |
| 7.78E-02 | 0.85 |
| 7.34E-02 | 0.97 |
| 6.77E-02 | 1.08 |
| 6.08E-02 | 1.20 |
| 5.31E-02 | 1.31 |
| 4.49E-02 | 1.43 |
| 3.65E-02 | 1.54 |
| 2.81E-02 | 1.65 |
| 2.02E-02 | 1.77 |
| 1.30E-02 | 1.88 |
| 7.12E-03 | 2.00 |
| 2.80E-03 | 2.11 |
| 4.28E-04 | 2.22 |

# FIGURES




a) RADSticker b) RADTriage

**Fig.1** Two commercially available SIRAD dosimeters



**Fig. 2** Photopgaph of the stamp-sized RADSticker placed at the center of a Uranium–glazed dish

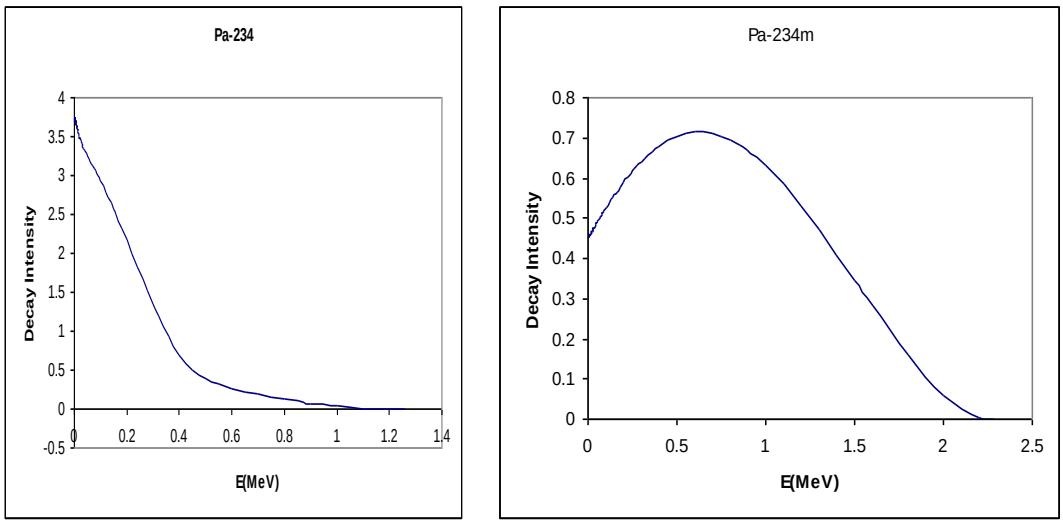



**Fig 3**: Beta spectrum of Protactinium $^{243}$Pa and $^{234m}$Pa

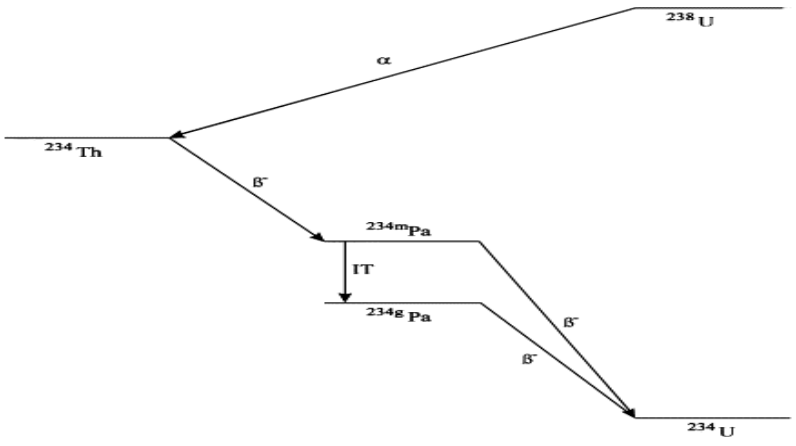



**Fig 4**: Partial decay chain of $^{238}$U

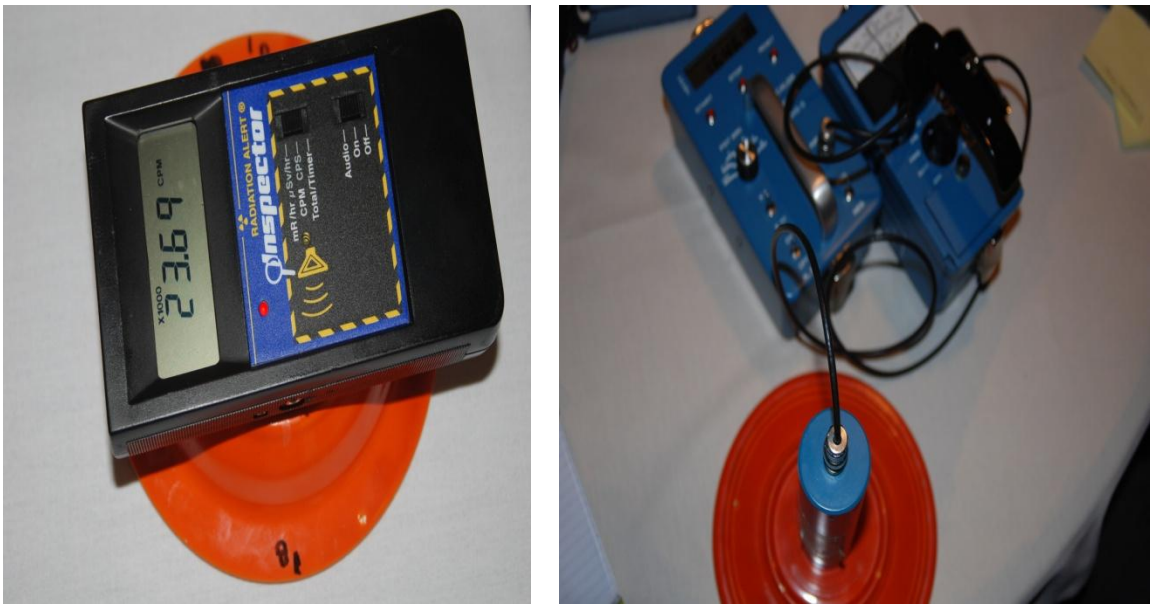



**Fig. 5** Picture of GM and NaI detector placed over uranium glaze

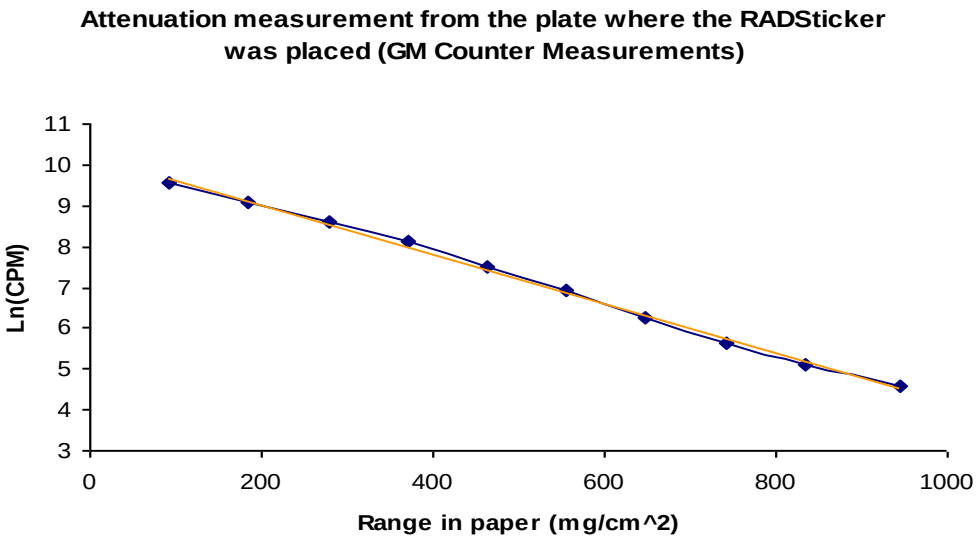



**Fig. 6a**) Beta absorption plot versus paper thickness, with GM placed over the thickness added to the plate.

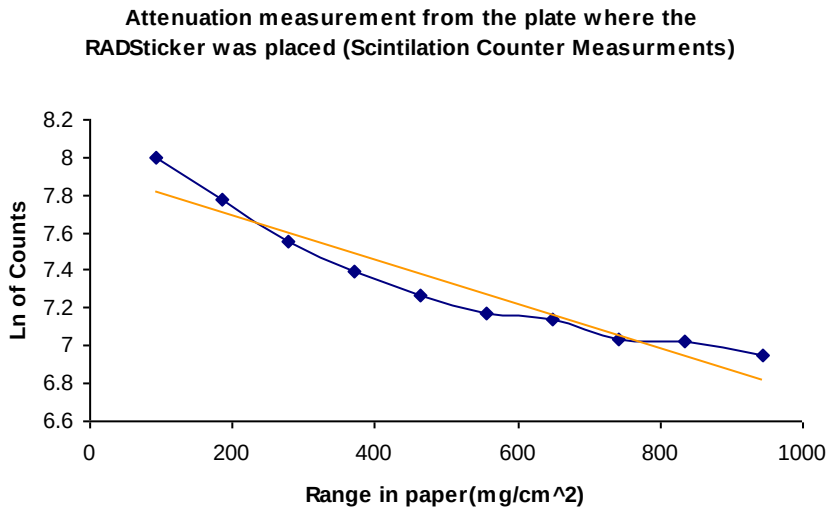



**Fig. 6b)** Beta absorption plot vs. paper thickness using NaI detector.

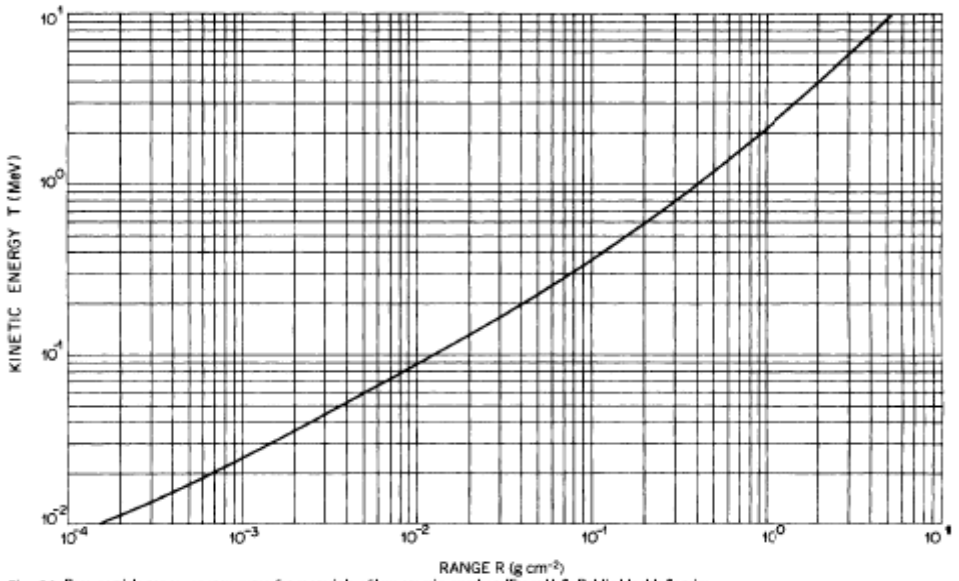



Fig. 6.4 Beta-particle range–energy curve for materials of low atomic number. [From U.S. Public Health Service, *Radiological Health Handbook*, Publ. No. 2016, Bureau of Radiological Health, Rockville, MD (1970).]

**Fig 7**: Range in low z material vs. electron energies from reference (from the

Radiological Health Handbook, Bureau of Radiological Health, 1970, as reprinted in Turner 2007)




a) RADSticker after 110 days b) RADTriage after 55 days

**Fig 8:** SIRAD dosimeters after exposure to beta radiation from Uranium glazed plates

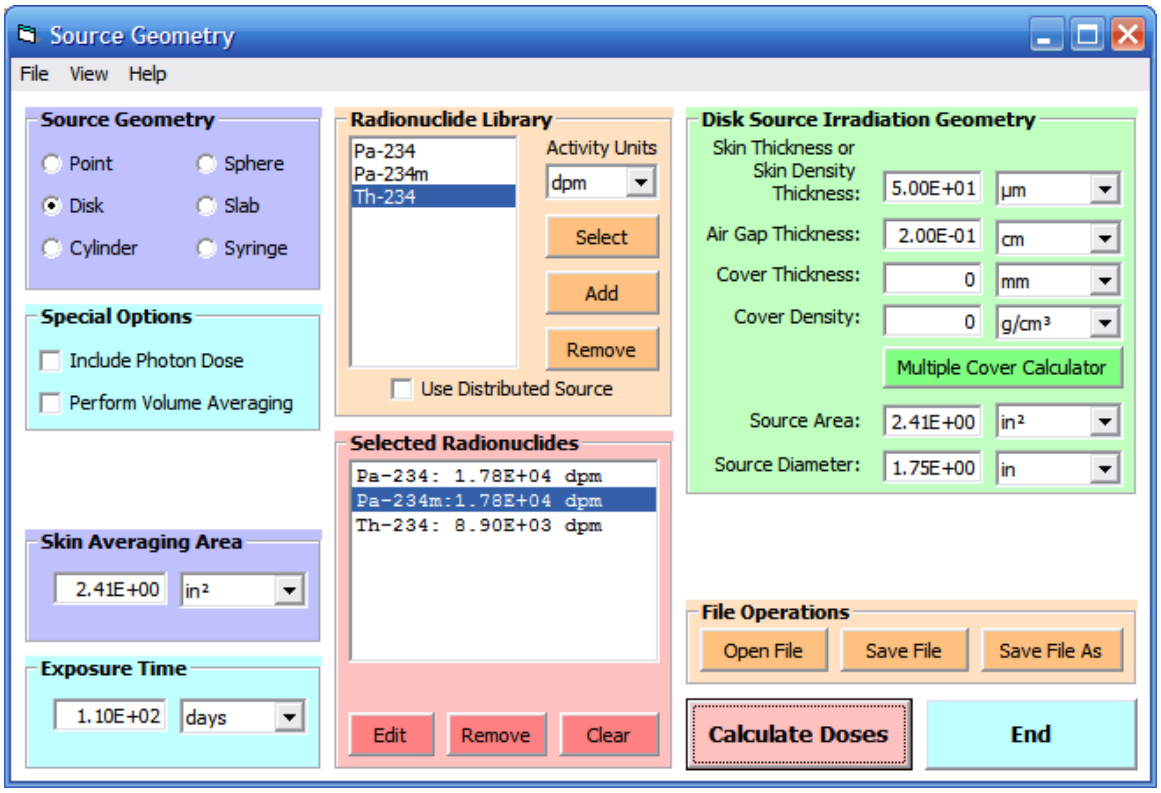



**Fig. 9a)** VARSKIN data input screeen

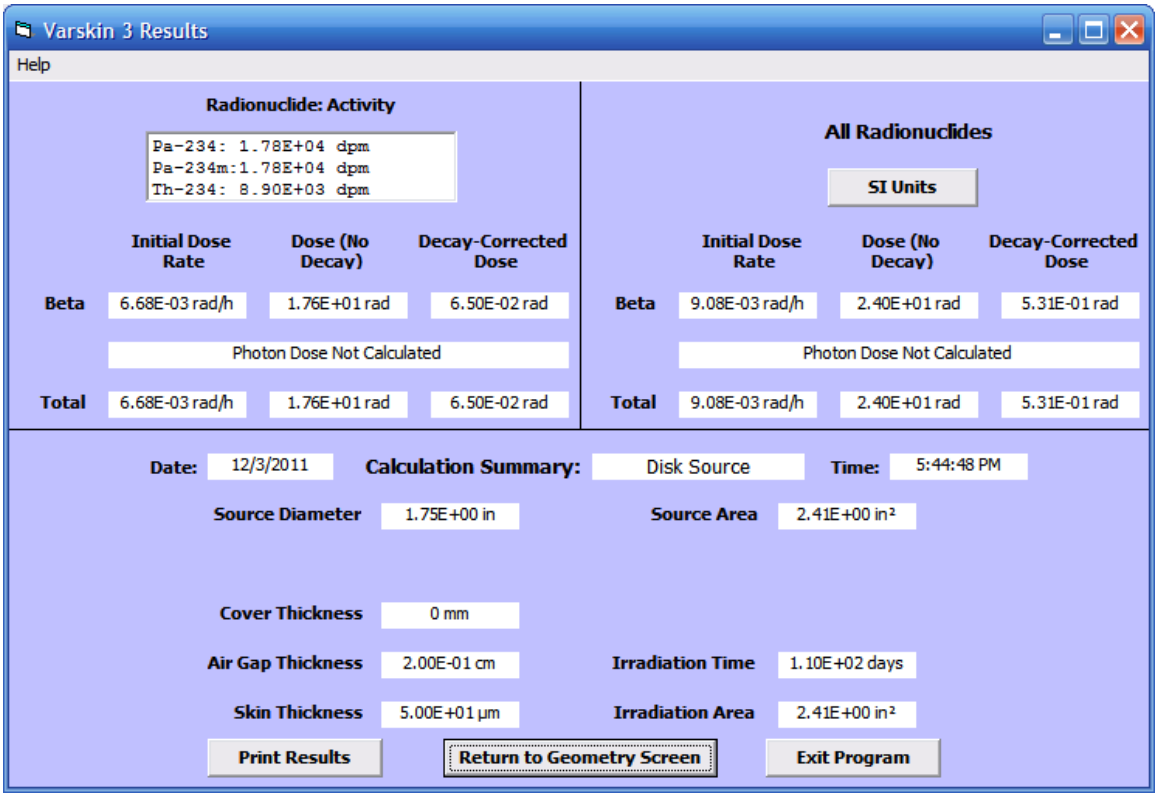
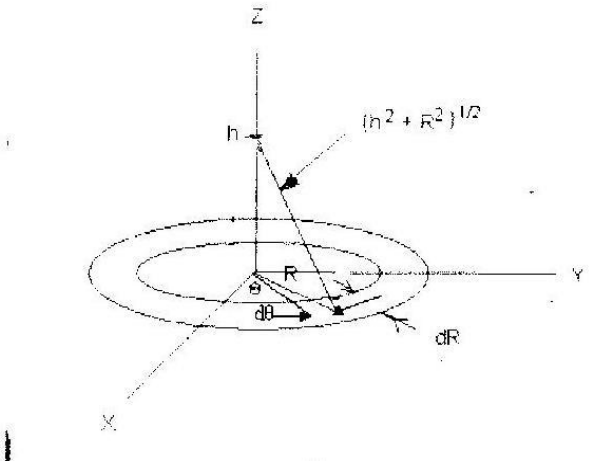



**Fig 9b)** VARSKIN output screen

# Exhibit A

The differential geometry for calculating the esu/cc air per hour (roentgen exposure rate) at height h above a plane uniformly contaminated with C microcuries per sq. cm, for radii R from one value to another, is the familiar form:




Let C = the surface concentration of activity in microcuries per square centimeter

Let SC(C) = the surface concentration in transformations per hour per square cm. Then,

$SC(C) := 2.22 \cdot 10^6 \cdot 60 \cdot C$ dis./hour per sq.cm

The linear energy absorption coefficient in $cm^{-1}$ is, for a gamma photon energy of 0.66 MeV:

$\mu en := 0.0294 \cdot 0.001293$ $\mu en = 3.801 \times 10^{-5}$

**Recalculation of above with GM window at h = 0.1 cm with wide angle incident electrons absorbed in the varying path through the RADSTicker backing (0.02 cm):**

$Rmax := 2.25$ Effective radius of GM open window, given by SE specs, close to U glaze.

$h := 0.1$ cm Assumed distance of GM from plate during measurement

$d := 0.02$

$$P(R) := \left[\left(h^2 + R^2\right)^{0.5}\right] \cdot \frac{d}{h}$$

$E(x) := interp(vEspl, vxR, vE, x)$

$$F := 16000 \cdot \frac{2}{\pi \cdot (2.38)^2} \qquad F = 1.798 \times 10^3$$

emission of betas per sq. cm per minute,assuming 50% geometry of GM measurements (high-sided)

$$DoseRate(h, F, Rmax) := \int_0^{Rmax} \int_0^{2 \cdot \pi} \left[ \int_{E\left[\left[\left(h^2+R^2\right)^{0.5}\right] \cdot \frac{d}{h}\right]}^{2200} \left[ pbeta(E) \cdot \left( spectMSP\left(\frac{E}{1000}\right)\right) \cdot \left[ F \cdot \frac{1}{4 \cdot \pi \cdot \left(R^2 + h^2\right)} \right] \right] dE \right] d\theta \, dR$$

## Dose for algorithm with skin absorption

**Using the actual exposure time of 110 days, between January 6 and April 26, 2011:**

$110 \cdot 24 \cdot 60 = 1.584 \times 10^{5}$ minutes $\qquad 110 \cdot 24 = 2.64 \times 10^{3}$ hours

$Dose110days := Radpermin \cdot 1.584 \cdot 10^{5} \qquad Dose110days = 60.412$ **rad**

**Going back to 0.007 cm thickness of dead layer of skin:** $d := 0.007 \quad h := 0.1$ (1 mm)

$$DoseRate(h,F,Rmax) := \int_{0}^{Rmax} \int_{0}^{2\cdot\pi} \left[ \int_{E\left[\left[\left(h^2+R^2\right)^{0.5}\right]\cdot\frac{d}{h}\right]}^{2200} \left[ pbeta(E)\cdot\left( spectMSP\left(\frac{E}{1000}\right)\right)\cdot\left[ F\cdot\frac{1}{4\cdot\pi\cdot\left(R^2+h^2\right)+2}\right]\right] dE \right] d\theta\, dR$$

$DoseRate(h,F,Rmax) = 5.437 \times 10^{3}$ MeV per gram of tissue per minute at P.

Rad per minute $\qquad Radpermin := DoseRate(h,F,Rmax)\cdot\frac{1.6\cdot 10^{-6}}{100} \qquad Radpermin = 8.699 \times 10^{-5}$

**Using the actual exposure time of 110 days, between January 6 and April 26, 2011:**

$110 \cdot 24 \cdot 60 = 1.584 \times 10^{5}$ minutes $\qquad Dose110days := Radpermin \cdot 1.584 \cdot 10^{5} \qquad Dose110days = 13.779$ **rad**

## References


Adsley I, Backhouse JS, Nichols AL, Toole J. U-238 decay chain: Resolution of observed anomalies in the measured secular equilibrium between Th-234 and daughter Pa-234m. Applied Radiation Isotopes, V 49, Issue 9-11; 1998, pp 1337-1344.

Berger MJ, Spencer LV. General Relation between fluxes from collimated point and plane sources of radiation. Phys. Rev; 1959, 113, 408-412

Berger MJ. Distribution of Absorbed dose around a point source of electrons and beta particles in water and other media. MIRD pamphlet No-7 J Nuclear Med 1971 Suppl. No.5,12.

Brodsky A, Beard GV. A compendium of information for use in controlling Radiation Emergencies, including Lecture Notes from a Training Session in Idaho Falls, ID, Feb 12- 14, ID 1958, ID-8206, U.S. Department of Energy, Idaho Operations Office, Idaho Falls, Idaho.

Brodsky A, Johnson RH Jr, Goans RE. Public protection from nuclear, biological and chemical terrorism. Medical Physics publishing; 2004, pp 684-691

Brodsky A. Personal Radiation Dose Monitor for the Public and emergency responders. Journal of American Physicians and Surgeons; Vol. 15 No-2, 2010

Buckley DW, Belanger R, Martin PE, Nicholaw KM, Swenson JB. Environmental assessment of consumer products Containing Radioactive Material; 1980 NUREG/CR-1775 SA 101380-469LJ/F

Buddemeier B. Self indicating instant radiation alert dosimeter (SIRAD) test results. Presented at the Fifty-Second Annual Meeting of the Health Physics Society; Vol. 93, July 2007, pp 8-12

Cember H. External beta-ray dosimetry. Chapter 4 in: Higginbotham J. Applications of New Technology: External Dosimetry, Health Physics Society; 1996 Summer School, Medical Physics Publishing, Madison, WI, 1996.

Cember H. Radiation Instruments, Health Physics 2001 Summer School, Medical Physics, Madison, Wisconsin, 2001.

Cross WG. Empirical Expression for beta ray point source Dose Distributions. Radiation protection Dosimetry; 1997, 69(2) : 85-96.

Durham J S. VARSKIN 3: NUREG/CR-6918 A computer Code for Assessing Skin Dose From Skin Dose Contamination, 2006, PP 38-40.

Durham JS. VARSKIN Mod 2 and SADDE Mod 2: computer codes for assessing skin dose from skin contamination 1992 Washington DC: US NRC NUREG/CR-5873/PNL-7913.

George V, Taplin MD, Clayton H, Douglas BS. A Colorimetric Dosimeter for Qualitative Measurement of Penetrating Radiations. Radiobiology 1951, Vol 56, 577-591.

IAEA. Summary Report on the Post-Accident Review Meeting on Chernobyl Accident. STI/PUB/740; 1986

ICRU. Journal Dosimetry of beta rays and low energy photons for brachytherapy with sealed sources. J ICRU; 2004; vol 4:21-8 .

IRCU Report. Dosimetry of external beta rays for radiation protection. Report; 56, 1997.

Johnson RH Jr, Googins SW. Radiation Instruments in University/Research laboratories and accelerators. Chapter 15 in: Cember H, Radiation Instruments, Health Physics 2001 Summer School, Medical Physics, Madison, Wisconsin; 2001.

Klemic G, Bailey P, Monetti M, Breheny C, Hall H, Buddemeier B. Self-Indicating Instant Radiation Alert Dosimeter (SIRAD) Test results Final Report. DHC/S&T/ SEDCMTB-2007-003, 2007.

Lewis HW. Multiple Scattering in an Infinite Medium. Phys. Rev; 1950, Vol 78, pp 526-529 .

Loevinger R, Japha EM, Brownell GM. Discrete radioisotope sources. Chapter 16 in: Hine GJ and Brownell GL, Editors, Radiation Dosimetry, Academic Press, Inc., New York, 1956, pp. 694-754.

Loevinger R. The Dosimetry of beta sources in tissue; the point-source function. Radiology; 1956, 66(1), pp 55-62.

NCRP Report. Limit for Exposure to Hot Particles on Skin, No. 106, 7910, 1989, pp. 27-28.

Piesch E, Burgkhardt B, Anton R. Dose rate measurement in the beta-photon Radiation field form $UO_2$ pellets and glazed ceramic containing Uranium. Radiation Protection Dosimetry; 1986 Vol-14, No-2, pp 109-112.

Riel GK, Winters P, Patel G, Patel P. Self-Indicating Radiation Alert Dosimeters (SIRAD). Radiation Protection Dosimetry; 2006 Vol. 120 No 1-4 PP 259-262.

Rossi BB and Staub HH. Ionization Chamber and Counters: Experimental Techniques; 1949.

Shapiro J. Radiation protection: A guide for scientists, regulators, and physicians; 2002, pp 225.

Sherbini S, DeCicco J, Gray AT, Struckmeyer R. Verification of the VARSKIN beta skin dose calculation computer code. Health Phys; 2008 94(6), 527-538.

Thomas JM, Bogard RS. Technical basis for beta skin dose calculations at the Y-12 Plant March 1994,U.S. DOE Y/DQ-51 DE-AC05-84OR21400.

Turner JE. Atoms, Radiation, and Radiation Protection; 2007 pp 466-468

Voss JT. Los Alamos Radiation Monitoring Notebook, 2011, PP-126